Article

Does the Oxygen Functionality Really Improve the Thermodynamics of Reversible Hydrogen Storage with Liquid Organic Hydrogen Carriers?

Sergey P. Verevkin [1,2,*] , Artemiy A. Samarov [3] and Sergey V. Vostrikov [4]

1   Competence Centre CALOR, Faculty of Interdisciplinary Research, University of Rostock,
    18059 Rostock, Germany
2   Department of Physical Chemistry, Kazan Federal University, 420008 Kazan, Russia
3   Department of Chemical Thermodynamics and Kinetics, Saint Petersburg State University, Peterhof,
    198504 Saint Petersburg, Russia; samarov@yandex.ru
4   Chemical-Technological Department, Samara State Technical University, 443100 Samara, Russia;
    vosser@mail.ru
*   Correspondence: sergey.verevkin@uni-rostock.de

Abstract: Liquid organic hydrogen carriers (LOHCs) are aromatic molecules that are being considered for the safe storage and release of hydrogen. The thermodynamic properties of a range of aromatic ethers were investigated using various experimental and theoretical methods to assess their suitability as LOHC materials. The absolute vapour pressures were measured for benzyl phenyl ether, dibenzyl ether and 2-methoxynaphthalene using the transpiration method. The standard molar enthalpies and entropies of vaporisation/sublimation were derived from the temperature dependence of the vapour pressures. The combustion energies of benzyl phenyl ether and dibenzyl ether were measured using high-precision combustion calorimetry, and their standard molar enthalpies of formation were derived from these data. High-level quantum chemical calculations were used to calculate the standard molar enthalpies of formation in the gas phase for benzyl phenyl ether, dibenzyl ether and 2-methoxynaphthalene. The latter values agreed very well with the experimental results obtained in this work. The thermodynamic properties of the hydrogenation/dehydrogenation reactions in liquid phase in LOHC systems based on methoxy–benzene, diphenyl ether, benzyl phenyl ether, dibenzyl ether and 2-methoxynaphthalene were derived and compared with the data for similarly structured hydrogen carriers based on benzene, diphenylmethane, 1,2-diphenylethane, 1,3-diphenylpropane and naphthalene. The influence of the oxygen functionality on the thermodynamic properties of the hydrogenation/dehydrogenation reactions was evaluated.

Keywords: hydrogen storage; LOHC; enthalpies of phase transitions; enthalpy of formation; vapour pressure; structure–property correlation; quantum-chemical calculations

1. Introduction

Hydrogen has proven to be a promising alternative to conventional fossil fuels and has the potential to solve the environmental and energy problems of the 21st century. As a clean and versatile energy carrier, hydrogen is the key to a sustainable and low-carbon future. However, the efficient and safe storage and transport of hydrogen remains a huge challenge. Liquid organic hydrogen carriers (LOHCs) have recently attracted much attention as a breakthrough solution to this challenge, revolutionising the way we handle and use hydrogen. LOHC is a fuel-like organic aromatic molecule that is loaded with hydrogen in a catalytic hydrogenation reaction [1]. The perhydrogenated product can be stored for an unlimited time and transported to the customer, and the hydrogen can be released on demand. From a chemical point of view, the LOHC system, therefore, consists of a pair of organic molecules, the hydrogen-lean (HL) form of the system (e.g., benzene, naphthalene,

etc.) and the hydrogen-rich (HR) form of the system (e.g., cyclohexane, decalin, etc.). An important aspect of all LOHC technologies is that the existing infrastructure of traditional fossil-fuel-based energy distribution technologies can generally be reused, which facilitates the establishment of the hydrogen economy.

Among the multitude of promising LOHCs, aromatic hydrocarbons are the most attractive from an economic point of view, although the dehydrogenation of these compounds is both kinetically and thermodynamically unfavourable. The high temperature of the methylcyclohexane/toluene system dehydrogenation process has led to a closer examination of other suitable polycyclic aromatic systems. Among the polycyclic compounds considered in the literature were decalin [2,3] bicyclohexyl, tercyclohexane [4], perhydroanthracene, perhydropyrene, perhydrofluorene, and perhydrofluoranthene [5], as well as hydrogenated forms of chrysene, picene, coronene and even hexabenzocoronene [6]. The gravimetric capacity, e.g., for the decalin/naphthalene system, is 7.2% wt. and 7.4% wt. for the perhydrocoronene/coronene system [7]. Of the compounds listed, decalin is the only one that is liquid under ambient conditions, while the other compounds are solids. As a rule, the aromatic counterparts of LOHC systems have high melting points, e.g., 148 °C for pyrene and 438 °C for coronene. To overcome this obstacle, it is necessary to use toluene to obtain a liquid, which reduces process safety. As an alternative, Pez et al. [6] suggested the use of compositions of two or more components that can form liquids or low-melting eutectic mixtures. The introduction of substituents, e.g., n-alkyl, alkoxyl or ether groups, into the ring structure of a polycyclic molecule also allows the melting point to be lowered, but the amount of hydrogen released decreases. According to Cooper et al. [8], compounds with high hydrogenation enthalpies generally require high dehydrogenation temperatures, and compounds with a large number of rings are characterised by relatively low hydrogenation enthalpies. Experimental data on the dehydrogenation of pentacene (73.2 kJ/mol H_2) and coronene (57.7 kJ/mol H_2) support this statement; however, for these compounds, it is shown that pentacene and coronene are able to release only 0.15 wt.% and 1 wt.%, respectively [9]. It has also been shown that π-conjugated aromatic molecules containing five-membered rings are more efficient hydrogen substrates because they have a lower enthalpy of dehydrogenation than the corresponding conjugated system in a six-membered ring. Decalin is an attractive carrier because it is liquid under normal conditions and has a high hydrogen capacity (7.2 wt%), with an energy density of 2.2 kWh/L. However, if toluene is used as a solvent, the capacity and energy density of the decalin/naphthalene system drop to 3.8 wt. % and 1.1 kWh/L, respectively [10]. In addition, the evaporation losses during storage are low due to the high boiling points, but the high temperature of the dehydrogenation reaction can lead to deactivation of the catalyst. A common disadvantage of the aromatic systems considered is the low selectivity in the dehydrogenation reaction phase caused by hydrocracking and hydrogenolysis reactions [7,10].

LOHC systems with oxygen functionality have been shown to offer very attractive hydrogen release performance at low temperatures and very attractive properties for potential technical applications [11]. For example, it has been shown that benzophenone can be selectively and completely hydrogenated to dicyclohexylmethanol over Ru/Al$_2$O$_3$ catalysts at 50 bar hydrogen pressure and temperatures in the range of 90 to 180 °C. Hydrogen can be released from dicyclohexylmethanol with Pt-based catalysts to recover benzophenon at a temperature of 250 °C. This reversible process is characterised by an excellent hydrogen storage capacity of 7.2 mass% [11]. This successful example has motivated further investigations of oxygen-containing LOHC systems. The focus of this work is the question of whether the introduction of oxygen functionality into aromatic molecules generally leads to an improvement in the thermodynamic properties of hydrogen storage compared to similarly shaped aromatic molecules without oxygen functionality.

It is known that the hydrogenation of aromatics is a thermodynamically favourable reaction. However, reversible dehydrogenation is thermodynamically unfavourable, and only the optimisation of the reaction conditions helps to shift the equilibrium towards a sufficient release of hydrogen. Understanding the general regularities between the

structures of LOHC counterparts and their thermodynamic properties is essential for screening molecules suitable for practical applications. Typical dehydrogenation reactions of hydrocarbon-based LOHCs and their analogues with oxygen functionality are shown in Figure 1.
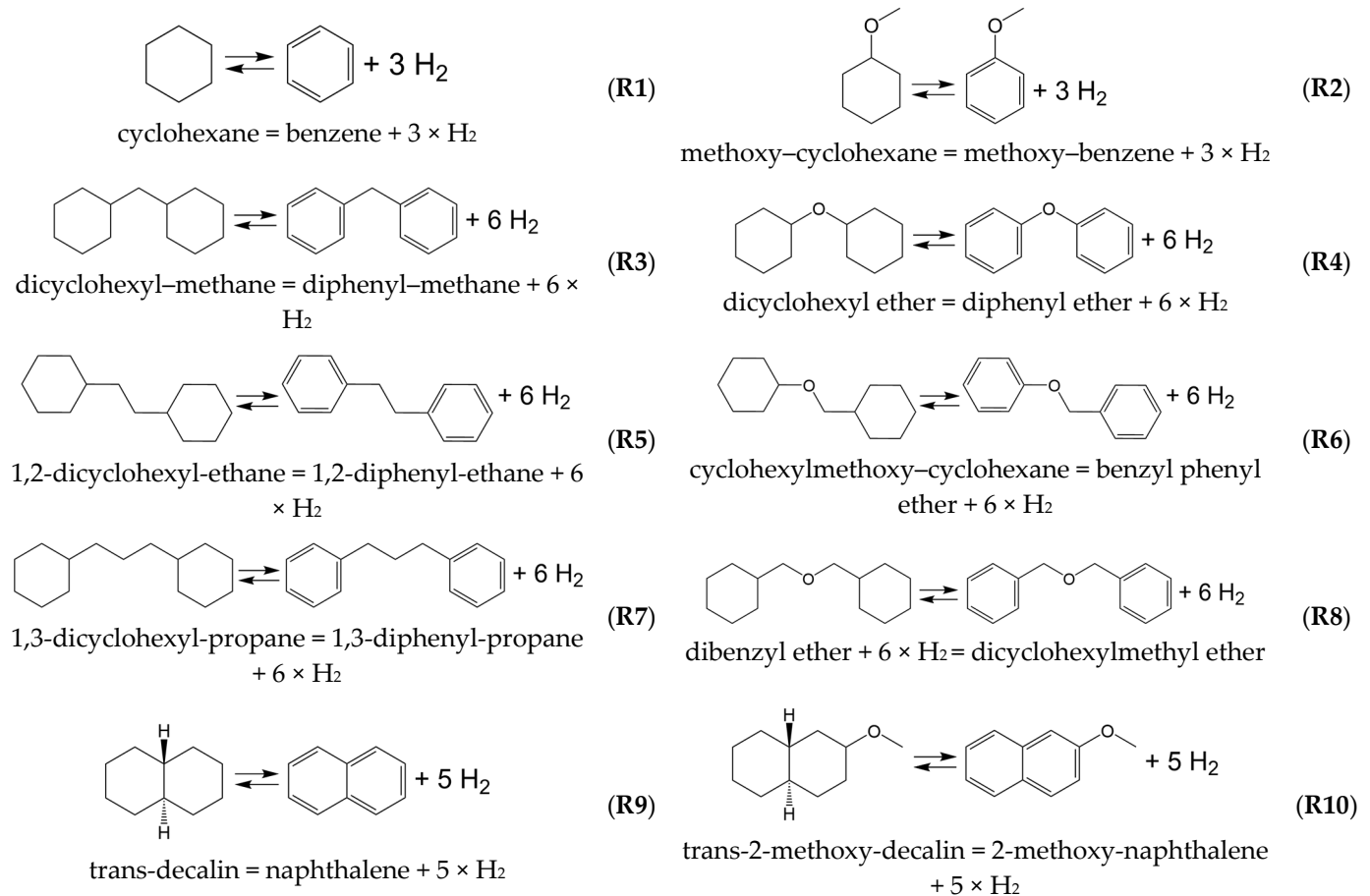

(R1) cyclohexane = benzene + 3 × H₂

(R2) methoxy–cyclohexane = methoxy–benzene + 3 × H₂

(R3) dicyclohexyl–methane = diphenyl–methane + 6 × H₂

(R4) dicyclohexyl ether = diphenyl ether + 6 × H₂

(R5) 1,2-dicyclohexyl-ethane = 1,2-diphenyl-ethane + 6 × H₂

(R6) cyclohexylmethoxy–cyclohexane = benzyl phenyl ether + 6 × H₂

(R7) 1,3-dicyclohexyl-propane = 1,3-diphenyl-propane + 6 × H₂

(R8) dibenzyl ether + 6 × H₂ = dicyclohexylmethyl ether

(R9) trans-decalin = naphthalene + 5 × H₂

(R10) trans-2-methoxy-decalin = 2-methoxy-naphthalene + 5 × H₂

Figure 1. The dehydrogenation reactions of liquid organic hydrogen carriers.

In this work, we carefully collected the available thermodynamic data for the HR and HL counterparts of the LOHC systems shown in Figure 1 and for related molecules. These data were evaluated by our own complementary measurements, structure–property correlations and high-level quantum chemical calculations and finally recommended for chemical engineering calculations.

The general feasibility of chemical reactions is determined by the sign and size of the standard Gibbs energy of the reaction, $\Delta_r G_m^o$, as follows (e.g., for a reaction in the ideal gas state):

$$\Delta_r G_m^o = \Delta_r H_m^o - T \times \Delta_r S_m^o = -RT \times \ln K_p \tag{1}$$

with $\Delta_r H_m^o$ = the standard molar reaction enthalpy, $\Delta_r S_m^o$ is the change in the standard molar entropy of a chemical reaction, and K_p = the gas-phase thermodynamic equilibrium constant. The Equation (1) is known as the Gibbs–Helmholtz equation, and it is broadly used in chemical engineering for the assessment of the K_p-values, which are directly related to the yield of the desired products of the reaction. The negative and large $\Delta_r G_m^o$ values provide evidence of a large thermodynamic driving force for the chemical reactions of interest. The standard Gibbs energy of reaction, $\Delta_r G_m^o$, is not directly measurable; therefore, it is calculated from the measurable enthalpic and entropic contributions involved in Equation (1). The standard molar reaction enthalpies, $\Delta_r H_m^o$, can be measured directly using reaction calorimetry or derived from temperature dependencies of equilibrium constants. However,

most frequently the $\Delta_r H_m^o$ values are calculated from the standard molar enthalpies of formation, $\Delta_f H_m^o$, of reaction participants. The change in the standard molar entropy of reactions, $\Delta_r S_m^o$, are generally derived from absolute entropies of reaction participants.

Given the countless molecules suitable for hydrogen storage, it is hardly possible to obtain the required thermodynamic properties for the numerous hydrogen-rich and hydrogen-poor counterparts of LOHC systems. The only way to collect sufficient data for thermodynamic analysis and optimisation of hydrogen storage is a clever combination of experimental and theoretical methods, including quantum chemical (QC) methods and empirical correlations of structural properties. In particular, the development of modern QC methods enables significant accumulation thermodynamics for the screening of promising LOHC systems since molar enthalpies of gas-phase formation calculated with QC high-level methods, $\Delta_f H_m^o$(g), nowadays reach a 'chemical accuracy' of $\pm(2–4)$ kJ·mol^{-1} for organic molecules with up to twenty heavy atoms in the structure [12].

The absolute gas-phase entropies, S_m^o(g), for molecules with moderate flexibility could also be calculated with a reasonable accuracy of $\pm(5–10)$ J·mol^{-1}·K^{-1} [13]. However, it should be noted that these achievements refer to the thermodynamic data of a single molecule in the ideal gas state. Progress in the development of QC methods for the calculation of properties in the liquid or crystalline state is still insufficient for the modelling of processes related to hydrogen storage.

Admittedly, hydrogen storage with the LOHC systems based on aromatic compounds is conveniently carried out in the liquid phase under a hydrogen pressure of up to 30 bar [1]. For such experimental conditions, the corresponding reaction enthalpies, $\Delta_r H_m^o$, required for Equation (1) are calculated from the liquid-phase standard molar enthalpies of formation of reactants, $\Delta_f H_m^o$(liq), using Hess's Law. The liquid phase $\Delta_r S_m^o$ values are also calculated from the corresponding liquid-phase entropies S_m^o(liq) of the reaction participants. Consequently, the equilibrium constant of the liquid phase, K_a, appears in Equation (1) instead of the thermodynamic equilibrium constant of the gas phase, K_p.

A valuable way of overcoming the limitations of QC methods and making them usable for the liquid phase is given by Equation (2):

$$\Delta_f H_m^o(\text{liq, 298.15 K}) = \Delta_f H_m^o(\text{g, 298.15 K})_{QC} - \Delta_l^g H_m^o(\text{298.15 K}) \qquad (2)$$

where $\Delta_f H_m^o$(g, 298.15 K)$_{QC}$ is the theoretical gas-phase enthalpy of formation calculated by any suitable high-level QC method, and $\Delta_l^g H_m^o$(298.15 K) is the standard molar enthalpy of vaporisation. There are numerous experimental methods to accurately measure $\Delta_l^g H_m^o$(298.15 K) values, and they can be relatively reliably estimated using various group additivity rules and structure–property correlations [14].

Similarly, the entropic contribution, S_m^o(liq, 298.15 K), to the Gibbs–Helmholtz equation (Equation (1)) can be derived by combining the QC and experimental methods as follows:

$$S_m^o(\text{liq, 298.15 K}) = S_m^o(\text{g, 298.15 K}) - \Delta_l^g S_m^o(\text{298.15 K}) \qquad (3)$$

where S_m^o(g, 298.15 K)$_{QC}$ is the theoretical gas-phase entropy calculated by any suitable high-level QC method and $\Delta_l^g S_m^o$(298.15 K) is the standard molar entropy of vaporisation, which can be derived from the slope of the temperature dependence of the experimental vapor pressures.

Such a combination of experimental and theoretical methods can greatly facilitate the screening of the promising LOHC and a reasonable workflow could be proposed to comprehensively determine the thermodynamic quantities essential for reversible hydrogen storage using Equation (1):

- *Step I*: The typical representatives of the promising LOHC systems are studied using the conventional experimental methods (the high-precision combustion calorimetry for $\Delta_f H_m^o$(liq/cr, 298.15 K) values and the transpiration method for $\Delta_l^g H_m^o$(298.15 K) and $\Delta_l^g S_m^o$(298.15 K) in this work)

- *Step II*: The high-level QC calculations are performed to derive $\Delta_f H_m^o$(g, 298.15 K)$_{QC}$ values and $\Delta_f S_m^o$(g, 298.15 K)$_{QC}$ values and the possible experimental and empirical methods are involved to validate these theoretical results.

- *Step III*: The liquid-phase $\Delta_f H_m^o$(liq, 298.15 K) and $\Delta_r S_m^o$(liq, 298.15 K) values are derived and used to calculate $\Delta_r G_m^o$(liq, *T*). In addition, the equilibrium constants are derived according to Equation (1), and a thermodynamic analysis of the LOHC system is carried out.

These steps represent the general roadmap of the present work, which aims to evaluate the impact and practical potential of introducing oxygen functionality in LOHC systems based on aromatic ethers compared to similarly structured aromatics.

2. Theoretical and Experimental Methods

Provenance and purities of the commercial sample of of benzyl phenyl ether, dibenzyl ether and 2-methoxy-napthalene are shown in Table S1. A high-precision self-made calorimeter equipped with a static bomb [15] was used for measurements of standard molar combustion energies of benzyl phenyl ether and dibenzyl ether. A transpiration method [16] was used to measure the vapor pressures over the solid and liquid samples of benzyl phenyl ether, dibenzyl ether, and 2-methoxy-napthalene. The temperature dependence of the absolute vapour pressures for each compound was used to derive the enthalpies and entropies of vaporisation of the aromatic ethers.

The melting temperature and enthalpy of fusion of benzyl phenyl ether were measured by DSC [17]. The main details of the experimental techniques are contained in the Supplementary Materials.

Quantum-Chemical Calculations

The conformational analysis was performed with a computer code called CREST (conformer-rotamer ensemble sampling tool). The software package uses a metadynamics simulation-based screening procedure to generate molecular conformations in the gas phase. A history-dependent bias potential is applied, where the collective variables for the metadynamics are the previous structures on the potential energy surface, expressed as the root-mean-square deviation of the atoms between them, which are calculated according to the quaternion algorithm. Conformations are generated at the GFNn-xTB level in the iMTD-GC workflow. More details are provided in the Ref. [18]. The obtained structures were optimised with the B3LYP/6–31 g(d,p) method [19]. It was found that the energetics of the conformers were quite close to each other within a few kJ·mol^{-1}. The most stable conformers for the aromatic compounds and their perhydrogenated products are shown in Figure S2.
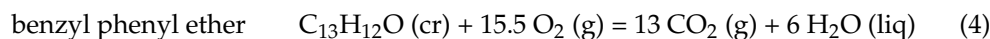
The Gaussian 16 series software [20] was used for QC calculations. The total H_{298}-enthalpies and the most stable conformers were calculated using the G3MP2 method [21]. The G3MP2 method was chosen as the optimal approach, combining high accuracy of energy calculation with reasonable computational cost. This method has been systematically used in our laboratory for calculations of C-, H-, N- and O-containing molecules, and in our experience, G3MP2 provides the theoretical enthalpies of formation in very good agreement with the reliable experimental values. The H_{298} values were finally converted to the theoretical $\Delta_f H_m^o$(g, 298.15 K)$_{QC}$ values and discussed. The well-established assumption "rigid rotator-harmonic oscillator" was used for the quantum-chemical calculations. The S_m^o(g, 298.15 K)$_{QC}$ values were calculated according to (Equation 1) using H_{298} and G_{298} from the output file. The general details of the calculation procedure have been published elsewhere [22].

3. Results and Discussion

3.1. Step I: Evaluation of Experimental and Empirical Thermochemical Results

3.1.1. Enthalpies of Formation from Combustion Calorimetry

The standard specific energies of combustion $\Delta_c u^o(cr)$ of benzyl phenyl ether and $\Delta_c u^o(liq)$ of dibenzyl ether were determined from five experiments for each compound. These $\Delta_c u^o(cr/liq)$ values were used to calculate the experimental standard molar enthalpies of combustion, $\Delta_c H_m^o$, which refer to the reactions:

benzyl phenyl ether $\quad$ $C_{13}H_{12}O$ (cr) + 15.5 O_2 (g) = 13 CO_2 (g) + 6 H_2O (liq) $\quad$ (4)

dibenzyl ether $\quad$ $C_{14}H_{14}O$ (liq) + 17 O_2 (g) = 14 CO_2 (g) + 7 H_2O (liq) $\quad$ (5)

The experimental standard molar enthalpies of combustion, $\Delta_c H_m^o$, were used to derive the standard molar enthalpies of formation in the crystal or liquid state $\Delta_f H_m^o(cr/liq)$ for both compounds. The results of combustion experiments are given in Table 1.

Table 1. Compilation of combustion results at T = 298.15 K (p° = 0.1 MPa) obtained for benzyl phenyl ether and dibenzyl ether [a].

Compound	$\Delta_c u^o(cr/liq)$	$\Delta_c H_m^o(cr/liq)$	$\Delta_f H_m^o(cr/liq)_{exp}$
	$J \cdot g^{-1}$	$kJ \cdot mol^{-1}$	$kJ \cdot mol^{-1}$
benzyl phenyl ether (cr)	$-36,691.3 \pm 5.1$	-6765.9 ± 2.4	-64.7 ± 3.0
dibenzyl ether (liq)	$-37,589.6 \pm 3.8$	-7459.9 ± 2.3	-50.0 ± 2.9

[a] Uncertainties related to the combustion experiments were estimated according to the procedure recommended by Olofsson [23]. The auxiliary information for the combustion experiments is given in Table S2.

The standard molar enthalpies of formation, $\Delta_f H_m^o(cr/liq)$, (see Table 1) were calculated based on the $\Delta_c H_m^o$ values of the reaction according to Equations (4) and (5) using Hess's Law and the standard molar enthalpies of formation of $H_2O(liq)$ and $CO_2(g)$ assigned by CODATA [24]. The total uncertainties of $\Delta_c H_m^o$ and $\Delta_f H_m^o$ values have been calculated according to the guidelines presented by Hubbard et al. [25] and Olofsson [23]. The uncertainties of combustion energies, $\Delta_c u^o(cr/liq)$, are expressed as the standard deviation of the mean. According to the thermochemical practice, the uncertainties assigned to the $\Delta_f H_m^o(cr/liq)$ values are twice the overall standard deviations and include the uncertainties of the calibration, the combustion energies of the auxiliary materials, and the uncertainties of the enthalpies of formation of the reaction products H_2O and CO_2. The combustion experiments with benzyl phenyl ether and dibenzyl ether were performed for the first time.

3.1.2. Absolute Vapour Pressures and Vaporisation Enthalpies

The primary vapour pressure–temperature dependencies for benzyl phenyl ether, dibenzyl ether and 2-methoxy-naphthalene measured in this work (see Table S3), and those from the literature (see Table S4) were fitted uniformly using a three-parametric equation (see ESI for details). From these data, the standard molar enthalpies of vaporisation at the respective temperatures T were derived. The final results at the reference temperature T = 298.15 K, $\Delta_l^g H_m^o(298.15 \text{ K})$, are summarised and compared in Table 2.

Only a few vapour pressure temperature dependencies of aromatic and aliphatic ethers relevant to this work can be found in the literature [26–28]. Furthermore, the enthalpies of vaporisation were never derived from these results. The available data for these compounds were collected and treated consistently in this work (see details in ESI) to calculate the $\Delta_l^g H_m^o(298.15 \text{ K})$ values in the same way as our own results from the transpiration method.

Table 2. Compilation of the standard molar enthalpies of vaporisation of aromatic and aliphatic ethers and hydrocarbons (in kJ·mol^{-1}).

Compounds	Method [a]	T-Range/ K	$\Delta_l^g H_m^o$ T_{av}	$\Delta_l^g H_m^o$ 298.15 K [b]	
benzyl phenyl ether 946-80-5	n/a	368.6–560.2	59.2 ± 1.0	71.3 ± 2.6	[26]
	T	318.3–363.2	70.6 ± 0.3	73.8 ± 0.4	Table S3
	BP	358–561	62.8 ± 0.6	74.7 ± 2.4	Table S4
				73.7 ± 0.5 [c]	average
	GA	298.15		75.8 ± 1.5	this work
dibenzyl ether 103-50-4	n/a	275–417	50.1 ± 1.0	(54.2 ± 1.3)	[27]
	n/a	413–561	57.4 ± 1.0	73.8 ± 3.4	[27]
	TGA	392–425	69.4 ± 1.0	78.9 ± 2.1	[28]
	T	309.4 ± 358.1	75.6 ± 0.4	78.6 ± 0.6	Table S3
	BP	365–571	67.0 ± 0.4	79.5 ± 2.5	Table S4
				78.5 ± 0.5	average
	GA	298.15		78.2 ± 1.5	this work
dicyclohexyl ether 4645-15-2	GA			68.3 ± 1.5	[29]
	BP	348–517	57.4 ± 1.1	68.1 ± 2.4	Table S4
				68.2 ± 1.3 [c]	average
1,2-diphenylethane 103-29-7	IP	333.2–413.2	64.0 ± 0.1	69.2 ± 1.0	[30]
	BP	338–558	59.6 ± 0.5	68.8 ± 1.9	Table S4
				69.1 ± 0.9 [c]	average
	GA	298.15		71.2 ± 1.5	this work
1,2-dicyclohexylethane 3321-50-4	BP	348–547	56.7 ± 0.8	68.2 ± 2.4	Table S4
	GA	298.15		67.2 ± 1.5	this work
	T_b	298.15		67.9 ± 2.0	Equation (6)
				67.6 ± 1.1 [c]	average
cyclohexylmethoxy–cyclohexane 118161-77-6	GA	298.15		69.7 ± 1.5	this work
1,3-diphenylpropane 1081-75-0	n/a	342–577	60.0 ± 1.0	71.4 ± 2.5	[27]
	SC	298.15		74.2 ± 2.0	[31]
	BP	342–576	63.4 ± 0.7	73.8 ± 2.2	Table S4
				73.3 ± 1.3	average
	GA	298.15		75.7 ± 1.5	this work
1,3-dicyclohexylpropane 3178-24-3	BP	382–565	58.1 ± 0.5	72.9 ± 3.0	Table S4
	GA	298.15		71.8 ± 1.5	this work
	T_b	298.15		71.3 ± 2.0	Equation (6)
				71.8 ± 1.1 [c]	average
dicyclohexylmethyl ether 14315-63-0	BP	356–574	59.2 ± 2.1	73.9 ± 3.6	Table S4
	GA	298.15		72.8 ± 1.5	this work
				73.0 ± 1.4 [c]	average
2-methoxy-naphthalene 93-04-9	BP	365–549	59.8 ± 1.1	68.9 ± 2.1	[32]
	T	348.2–378.2	65.4 ± 0.8	69.1 ± 0.9	[32]
	T	348.7–372.4	66.1 ± 0.5	69.6 ± 0.6	Table S3
	PhT			69.2 ± 0.8	Table S5
				69.4 ± 0.4 [c]	average
2-methoxy-decalin (liq) 55473-38-6	GA			58.4 ± 1.0	[32]
	T_b			58.8 ± 1.0	[32]
	BP	349–509	49.6 ± 1.7	58.7 ± 2.5	Table S4
				58.6 ± 0.7 [c]	average

[a] Methods: n/a = method is not available; T = transpiration method; SC = solution calorimetry; T_b = from correlation with the normal boiling temperatures; BP = estimated from boiling points at different pressures (see Table S4); PhT = from the consistency of phase transitions (see Table S5); GA = calculated according to the group additivity (see text). [b] Vapour pressures available in the literature were treated using Equations (S2) and (S3) with the help of heat capacity differences from Tables S6 and S7 to calculate the enthalpies of vaporisation at 298.15 K. Uncertainties of the sublimation/vaporisation enthalpies $U(\Delta_l^g H_m^o)$ are the expanded uncertainties (0.95 level of confidence). They include uncertainties from the fitting equation and uncertainties from temperature adjustment to T = 298.15 K. Uncertainties in the temperature adjustment of vaporisation enthalpies to the reference temperature T = 298.15 K are estimated to account for 20% of the total adjustment. [c] Weighted mean value (uncertainties were taken as the weighting factor). Values given in bold are recommended for further thermochemical calculations.

The results show that no systematic vapour pressure measurements were available for most of the hydrogenated aromatic ethers. However, the experimental boiling points (BP) of the desired aliphatic cyclic ethers at different reduced pressures can be found in the literature (see a compilation in Table S4) and may be helpful in obtaining the missing thermodynamic information. These boiling points usually originate from the distillation of reaction mixtures after synthesis and are generally only used to identify the compounds. In such experiments, the pressures are usually measured with uncalibrated manometers, and the temperatures are given in the range of a few degrees. However, our previous work (e.g., on methylbiphenyls [33]) has shown that, in general, reasonable trends can be derived even from such rough data. This general conclusion also applies to the aromatic ethers. As shown in Table 2, the $\Delta_l^g H_m^o$(298.15 K) values for benzyl phenyl ether and dibenzyl ether derived from BP at various reduced pressures agree with the enthalpies of vaporisation measured by conventional methods within the experimental uncertainties.

Therefore, we carefully collected and evaluated the available thermodynamic data and BP for all reactions R1 to R10 in Figure 1 from the literature and used these data to calculate their $\Delta_l^g H_m^o$(298.15 K) and $\Delta_l^g S_m^o$(298.15 K) values (see Tables S3 and S4), which are required for the thermodynamic analysis of the dehydrogenation reactions shown in Figure 1.

As shown in Figure 1, the thermodynamics of the dehydrogenation of aromatic ethers are compared with those of similarly structured aromatic hydrocarbons and their fully dehydrogenated aliphatic counterparts. While reliable experimental data from the literature are available for the pairs benzene and cyclohexane, diphenyl–methane and dicyclohexyl–methane, naphthalene, and decalin (see Table 2), the thermodynamic data for the pairs 1,2-diphenyl-ethane and 1,2-dicyclohexyl-ethane, 1,3-diphenyl-propane, and 1,3-dicyclohexyl-propane were evaluated in this work (see Table 2) and these data were recommended for thermochemical calculations.

3.1.3. Validation of Vaporisation Enthalpies by Structure–Property Correlations

Structure–property correlations are the backbone of physical–organic chemistry, as the new experimental results are integrated into the network of already known and evaluated data. Provided that the new results are consistent with the trends already known from the available results, they can be recommended for the thermochemical calculations. If this is not the case, the unusual structural effects could be anticipated, or the measurements should be repeated to avoid confounding. In this context, before using $\Delta_l^g H_m^o$(298.15 K) values derived from single experiments using conventional methods or from BP, it is useful to validate the results by structure–property correlations, e.g., with relationships between the enthalpy of vaporisation and normal boiling points (T_b). For example, in our recent work [34], a robust $\Delta_l^g H_m^o$(298.15 K)$-T_b$ relationship was established for a large series of alkyl-cyclohexanes:

$$\Delta_l^g H_m^o(298.15 \text{ K}) = 0.1972 \times T_b - 37.6 \text{ with } R^2 = 0.989 \qquad (6)$$

We used this correlation to assess the $\Delta_l^g H_m^o$(298.15 K)-values for 1,2-dicyclohexyl-ethane and 1,3-dicyclohexyl-propane, and the results (see Table 2, indicated as T_b) agreed very well with the vaporisation enthalpies derived from the approximation of BP selected in Table S4.

Group additivity (GA) methods are another valuable way of correlating structural properties. These methods are generally based on the idea of the Lego box, where a property of a molecule is assembled from small building blocks with well-established numerical contributions. Comprehensive systems of group contributions (or increments) have been developed for most major classes of organic compounds [14]. The set of group contributions used in this work for the prediction of thermodynamic properties is listed in Table S8. However, it is well known that the conventional GA methods have difficulties with cyclic molecules. To improve the quality of the prediction, numerous and unique 'ring' corrections are proposed [14,35]. However, for the molecules investigated in this work, it might be more practical to use a phenyl fragment (C_6H_{5-}) and a cyclohexyl fragment

(C$_6$H$_{11}$-) developed as shown in Figure S1 instead of the 'ring' corrections. These fragments were used to calculate the thermodynamic properties of aromatic and aliphatic ethers and hydrocarbons and their hydrogenated counterparts. The examples of GA calculations for the LOHC pairs dibenzyl ether/dicyclohexylmethyl ether and 1,3-diphenylpropane/1,3-dicyclohexylpropane are shown in Figure 2.
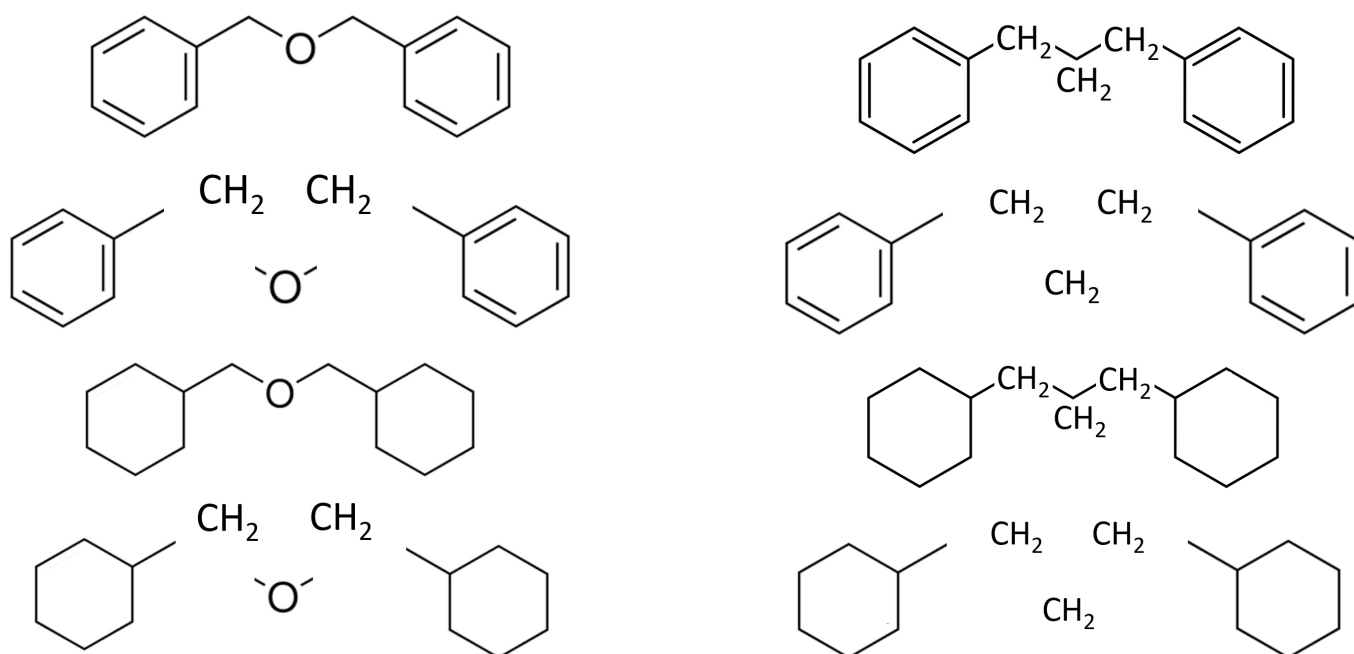

Figure 2. Calculating the enthalpy of vaporisation, $\Delta_l^g H_m^o$(298.15 K) or $\Delta_f H_m^o$(g, 298.15 K) of for LOHC pairs dibenzyl ether/dicyclohexylmethyl ether and 1,3-diphenyl-propane/1,3-dicyclohexyl-propane. The numerical values of contributions required for calculations are given in Table S8.

The results of the GA calculations are summarised in Table 2. For all aromatic and aliphatic compounds, the enthalpies of vaporisation $\Delta_l^g H_m^o$(298.15 K) evaluated in this way are in good agreement with results obtained using other methods. To gain more confidence in the enthalpies of vaporisation, the weighted average values were calculated for each species considered in this work (see Table 2) and used to calculate the enthalpies of formation of the liquid phase in Section 3.3

3.2. Step II: Quantum-Chemical Calculations of the Gas-Phase Enthalpies of Formation

The aromatic and aliphatic ethers are flexible molecules and are represented in the gas phase by a mixture of conformers. The energies E_0 and the total enthalpies H_{298} of the most stable conformers were finally calculated using the method G3MP2 implemented in the software Gaussian 16. The resulting H_{298} enthalpies were converted to the standard molar enthalpies of formation based on conventional atomisation (AT) procedure [22] (e.g., for benzyl phenyl ether):

$$C_{13}H_{12}O \rightarrow 13 \times C + 12 \times H + 1 \times O \tag{7}$$
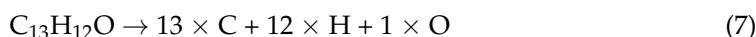
The results of the quantum chemical G3MP2 calculations for the hydrogen-lean and hydrogen-rich counterparts of the LOHC systems are summarised in Table 3 (column 3).

Table 3. Results of quantum-chemical calculations with the G3MP2 method for aromatic compounds and their hydrogenated products at T = 298.15 K (p° = 0.1 MPa). All data are in kJ·mol^{-1}.

CAS	Compound	$\Delta_f H_m^o$(g, AT)$_{G3MP2}$ [a]	$\Delta_f H_m^o$(g)$_{exp}$ [b]	$\Delta_f H_m^o$(g)$_{QC}$ [c]	Δ [d]
496-16-2	dihydrobenzofuran	−57.5	−47.0 ± 1.4 [36]	−46.3	−0.7
496-14-0	dihydroisobenzofuran	−36.9	−30.1 ± 1.0 [37]	−25.3	−4.8
493-05-0	isochromane	−78.2	−63.1 ± 1.1 [38]	−67.4	4.3
2216-69-5	1-methoxynaphthalene	−19.0	−6.7 ± 1.8 [32]	−7.1	0.4
93-04-9	2-methoxynaphthalene	−20.3	−6.5 ± 1.4 [32]	−8.4	1.9
493-08-3	dihydrobenzopyran	−96.2	−82.4 ± 1.2 [38]	−85.8	3.4
21720-89-8	1-methoxydecalin	−333.6	−328.7 ± 3.5 [32]	−327.8	−0.9
55473-38-6	2-methoxydecalin	−334.6	−329.5 ± 3.5 [32]	−328.8	−0.7
101-84-8	diphenyl ether	38.6	50.9 ± 1.4 [29]	51.6	−0.7
4645-15-2	dicyclohexyl ether	−361.4	-	**−356.1**	
946-80-5	phenyl benzyl ether	20.7	30.6 ± 3.1 [Table 4]	33.4	−2.8
118161-77-6	cyclohexylmethoxy–cyclohexane	−377.0	-	**−372.0**	
103-50-4	dibenzyl ether	15.0	28.5 ± 3.0 [Table 4]	27.6	0.9
14315-63-0	dicyclohexylmethyl ether	−391.5	-	**−386.8**	

[a] Calculated by G3MP2 and atomisation reaction with the expanded uncertainties of ±4.1 kJ·mol^{-1} [21]. [b] Uncertainties in this table are expressed as two times the standard deviation. [c] Calculated according to Equation (8). [d] Difference between column 3 and column 4.

Admittedly, the AT reaction to convert the resulting H_{298} enthalpies to the standard molar enthalpies of formation is the least biased choice compared to other isodesmic, iso-gyric, homodesmotic, etc., reactions [39]. The main advantage of the AT reaction is that the enthalpies of the atoms are precisely known, compared to the less precise enthalpies of the formation of the various molecules involved in the construction of the aforementioned reactions. However, it is also known [36,39] that the QC results calculated with the G3MP2 and the AT reactions, $\Delta_f H_m^o$(g, AT), show a small but noticeable deviation from the experimental results (see Table 3). Nevertheless, a simple correction derived from a set of similarly structured molecules with reliable experimental enthalpies of formation, $\Delta_f H_m^o$(g)$_{exp}$, (see Table 3, Tables S10 and S11) can reconcile QC and experimental results if the $\Delta_f H_m^o$(g, AT) values are correlated with the experimental values. The following equation,

$$\Delta_f H_m^o(g)_{QC}/\text{kJ·mol}^{-1} = 1.0194 \times \Delta_f H_m^o(g, AT)_{G3MP2} + 12.3 \qquad \text{with} R^2 = 0.9996 \quad (8)$$

was used to obtain the "corrected" QC results for the aromatic ethers and their hydro-genated products. The correction for 1,2-diphenyl ethane and 1,3-diphenyl-propane was made with the following equation:

$$\Delta_f H_m^o(g)_{QC}/\text{kJ·mol}^{-1} = 0.9576 \times \Delta_f H_m^o(g, AT)_{G3MP2} + 18.5 \qquad \text{with} R^2 = 0.9979 \quad (9)$$

which was derived from the data for similarly structured alkyl-biphenyls (see Table S10). For their hydrogenated products, the following equation was applied:

$$\Delta_f H_m^o(g)_{QC}/\text{kJ·mol}^{-1} = 0.970 \times \Delta_f H_m^o(g, AT)_{G3MP2} - 3.2 \quad \text{with} R^2 = 0.9998 \quad (10)$$

derived from the data for similarly structured alkyl-cyclohexanes (see Table S11). It is obvious that the coefficients of Equations (8) to (10) are slightly different because the ele-mentary compositions of the molecules in the sets are different, as well as the structures of the molecules included in the sets (e.g., aromatic molecules in Table S10 and aliphatic molecules in Table S11). The enthalpies of formation calculated with the corrected atom-isation reactions are given in Table 3, column 5, and used for further thermochemical calculations (see Section 3.3).

The QC results for benzyl phenyl ether, dibenzyl ether and 2-methoxy-naphthalene were validated with the experimental values evaluated in Table 4.

Table 4. Comparison of experimental and theoretical thermochemical data at T = 298.15 K (p° = 0.1 MPa) for aromatic ethers (in kJ·mol^{-1}) [a].

Compound	$\Delta_f H_m^o$(cr/liq)$_{exp}$ [b]	$\Delta_{cr/l}^g H_m^o$ [c]	$\Delta_{cr}^l H_m^o$ [d]	$\Delta_f H_m^o$(g)$_{exp}$ [e]	$\Delta_f H_m^o$(g)$_{QC}$ [f]
benzyl phenyl ether (cr)	-64.7 ± 3.0	73.7 ± 0.5	21.6 ± 0.4	30.6 ± 3.1	33.4 ± 4.1
dibenzyl ether (liq)	-50.0 ± 2.9	78.5 ± 0.5		28.5 ± 3.0	27.6 ± 4.1
2-methoxy-naphthalene (cr)	-96.6 ± 1.3 [32]	90.1 ± 0.5 [32]		-6.5 ± 1.4	-8.4 ± 4.1

[a] Uncertainties correspond to expanded uncertainties of the mean (0.95 level of confidence). [b] From Table 1. [c] The evaluated values from Table 2. [d] From Table S5. [e] The sum of columns 2 to 4. [f] Calculated with the G3MP2 method using the corrected atomisation reactions (see Table 3, column 5).

3.3. Step III: Thermodynamic Analysis of the LOHC Systems

3.3.1. Comparison of the Energetics of Dehydrogenation Reactions with and without Oxygen Functionality

The standard molar enthalpies of chemical reactions were calculated from the standard molar enthalpies of formation, $\Delta_f H_m^o$, of the reactants according to Hess´s Law:

$$\Delta_r H_m^o(T) = \sum[\Delta_f H_m^o(T, \text{ products})] - \sum[\Delta_f H_m^o(T, \text{ educts})] \qquad (11)$$

Unfortunately, $\Delta_f H_m^o$ values for some cyclic aliphatic molecules of the hydrogen-proximal LOHC counterparts of the R1–R10 reactants are missing in the literature. However, they can be reliably calculated at a high level using QC methods, as shown in our recent work for the series of alkyl-cyclohexanes [34]. Therefore, we calculated the missing gas-phase formation enthalpies of aromatic ethers, aromatic hydrocarbons and their perhydrogenated counterparts with G3MP2 (see Table 3, column 5) and converted them into the liquid-phase formation enthalpies by subtracting the enthalpies of vaporisation as shown in Equation (2). The required $\Delta_l^g H_m^o$(298.15 K) contributions in Equation (2) for aromatic and hydrogenated LOHC counterparts were already evaluated in Table 2. The $\Delta_f H_m^o$(liq, 298.15 K) values, derived according to Equation (2), are given in Table 5 and can now be used as input to Hess´s Law (Equation (11)).

Table 5. Compilation of thermochemical data at T = 298.15 K (p° = 0.1 MPa) for LOHC counterparts (in kJ·mol^{-1}) [a].

Compound; CAS	$\Delta_f H_m^o$(g) [b]	$\Delta_l^g H_m^o$ [c]	$\Delta_f H_m^o$(liq) [d]
diphenyl–methane; 101-81-5	164.7 ± 0.9 [40]	68.1 ± 0.3 [40]	96.6 ± 0.8 [40]
dicyclohexyl–methane; 3178-23-2	-242.4 ± 2.0 [34]	64.7 ± 1.0 [34]	-307.1 ± 2.2 [34]
diphenyl ether, 101-84-8	50.9 ± 1.4 [29]	66.7 ± 0.2 [29]	-15.8 ± 1.4 [29]
dicyclohexyl ether; 4645-15-2	-356.1 ± 4.1 [Table 3]	68.2 ± 1.3	-424.3 ± 4.3
1,2-diphenyl-ethane; 103-29-7	133.7 ± 4.1 [Table S10]	69.1 ± 0.9	64.6 ± 4.2
1,2-dicyclohexyl-ethane; 3321-50-4	-261.0 ± 4.1 [Table S11]	67.6 ± 1.1	-328.6 ± 4.2
benzyl phenyl ether; 946-80-5	30.6 ± 3.1 [Table 4]	73.7 ± 0.5	-43.1 ± 3.1
cyclohexylmethoxy–cyclohexane; 118161-77-6	-372.0 ± 4.1 [Table 3]	69.7 ± 1.5	-441.7 ± 4.4
1,3-diphenyl-propane; 1081-75-0	114.7 ± 4.1 [Table S10]	73.3 ± 1.3	41.4 ± 4.3
1,3-dicyclohexyl-propane; 3178-24-3	-281.6 ± 4.1 [Table S11]	71.8 ± 1.1	-353.4 ± 4.2
dibenzyl ether; 103-50-4	-50.0 ± 2.9 [Table 4]	78.5 ± 0.5	-128.5 ± 2.9
dicyclohexylmethyl ether; 14315-63-0	-386.8 ± 4.1 [Table 3]	73.0 ± 1.4	-459.8 ± 4.3
naphthalene; 91-20-3	150.6 ± 1.5 [41]	55.4 ± 1.4 [41]	94.9 ± 1.6 [41]
trans-decalin; 493-02-7	-182.0 ± 1.0 [42]	48.6 ± 0.2 [42]	-230.6 ± 1.0 [42]
2-methoxy-naphthalene; 93-04-9	-6.5 ± 1.4 [32]	69.4 ± 0.4	-75.9 ± 1.5
trans-2-methoxy-decalin; 55473-38-6	-329.5 ± 3.6 [32]	58.6 ± 0.7	-388.1 ± 3.6

[a] Uncertainties correspond to expanded uncertainties of the mean (0.95 level of confidence). [b] Calculated with the G3MP2 method using the corrected atomisation reactions (see Table 3, Tables S10 and S11) or taken from the original literature. [c] From Table 2 or from original literature. [d] Calculated as the difference between columns 2 and 3 in this table.

The results of the calculation of the liquid-phase reaction enthalpies, $\Delta_r H_m^o(\text{liq})$, of the dehydrogenation reactions R1 to R10 are shown in Table 6.

Table 6. Calculation of the liquid-phase reaction enthalpies, $\Delta_r H_m^o(\text{liq})$, of the dehydrogenation reactions R1 to R10 in Figure 1, at T = 298.15 K (p^o = 0.1 MPa, in kJ·mol^{-1}).

Compound	$\Delta_f H_m^o(\text{liq})_{HL}$ [a]	$\Delta_f H_m^o(\text{liq})_{HR}$ [b]	$\Delta_r H_m^o(\text{liq})$ [c]	$\Delta_r H_m^o(\text{liq})/\text{H}_2$ [d]
benzene	49.0 ± 0.9 [Table S12]	−156.4 ± 0.8 [Table S12]	205.4	68.5
methoxy–benzene	−116.9 ± 0.7 [Table S12]	−313.7 ± 3.5 [Table S12]	196.8	65.6
diphenyl–methane	96.6 ± 0.8	−307.1 ± 2.2	403.7	67.3
diphenyl ether	−15.8 ± 1.4	−424.3 ± 4.3	408.5	68.1
1,2-diphenyl-ethane	64.6 ± 4.2	−328.6 ± 4.2	393.2	65.5
benzyl phenyl ether	−43.1 ± 3.1	−441.7 ± 4.4	398.6	66.4
1,3-diphenyl-propane	41.4 ± 4.3	−353.4 ± 4.2	394.8	65.8
dibenzyl ether	−50.0 ± 2.9	−459.8 ± 4.3	409.8	68.3
naphthalene	94.9 ± 1.6	−230.6 ± 1.0	325.5	65.1
2-methoxy-naphthalene	−75.9 ± 1.5	−388.1 ± 3.6	312.2	62.4

[a] Liquid-phase enthalpies of formation of of aromatic ethers and hydrocarbons (hydrogen-lean (HL) counterparts of the LOHC system) from Table 5. [b] Liquid-phase enthalpies of formation of perhydrogenated aromatic ethers and hydrocarbons (hydrogen-rich (HR) counterparts of the LOHC system) from Table 5. [c] Calculated according to Hess´s Law applied to the reactions R1 to R10 shown in Figure 1. [d] Reaction enthalpy per mole H$_2$.

As can be seen from this table, the reactions R1 to R10 are strongly endothermic from 196.8 to 409.8 kJ·mol^{-1}. However, it should be noted that different numbers of hydrogen molecules are involved in these reactions. Therefore, the enthalpy of the reaction is usually related to the amount of hydrogen released as a kJ·mol^{-1}/$_{H2}$ unit in order to be able to correctly compare the energetics of hydrogenation reactions, taking the stoichiometry into account. As can be seen from Table 6, the dehydrogenation enthalpies in these units are generally at the level of $\approx$65 kJ·mol^{-1}/$_{H2}$ for all pairs. In general, the lower the reaction enthalpy, the better and more effective the dehydrogenation process is from a thermodynamic point of view. According to the results shown in Table 6, the influence of oxygen functionality is favourable for the cyclohexane/benzene, methoxy–cyclohexane/methoxy–benzene, and 2-methoxy-decalin/2-methoxy-naphthalene pairs. For other LOHC pairs, the influence is quite small, and even the dehydrogenation of oxygenated cycloalkanes is somewhat less thermodynamically favoured compared to the aliphatic hydrocarbons.

3.3.2. Comparison of the Reaction Entropies of Dehydrogenation of Lohc Based on Ethers and Hydrocarbons

The liquid-phase standard molar entropies, $S_m^o(\text{liq}, 298.15\text{ K})$, were calculated according to Equation (3) using the gas-phase standard molar entropies $S_m^o(\text{g}, 298.15\text{ K})$ from G3MP2 calculations and the standard molar entropy of vaporisation, $\Delta_l^g S_m^o(298.15\text{ K})$, derived (details are given in ESI) from the intercept of the temperature dependencies of the experimental vapor pressures. The results for $\Delta_l^g S_m^o(298.15\text{ K})$, $S_m^o(\text{g}, 298.15\text{ K})$, and final entropies, $S_m^o(\text{liq}, 298.15\text{ K})$, are shown in Table 7.

$$\Delta_r S_m^o(T) = \sum[S_m^o(T, \text{ products})] - \sum[S_m^o(T, \text{ educts})] \tag{12}$$

The resulting total liquid-phase reaction entropies, $\Delta_r S_m^o(\text{liq}, 298.15\text{ K})$, of the dehydrogenation reactions R1 to R10 are given in Table 8, column 3.

Table 7. Compilation of the standard molar entropies of vaporisation, $\Delta_l^g S_m^o$, and the absolute standard molar entropies, S_m^o(g or liq), of reactants of reactions R1–R10 (all values at T = 298.15 K in J·mol^{-1}·K^{-1}).

Compound	$\Delta_l^g S_m^o$ [a]	S_m^o(g) [b]	S_m^o(liq) [c]
benzene			173.3 [43]
methoxy–benzene	111.8 ± 0.1 [44]	346.6	234.8
diphenyl–methane	140.5± 0.5 [45]	440.3	299.8
diphenyl ether	134.5± 4.3 [29]	439.8	305.3
1,2-diphenyl-ethane	134.9 ± 1.8	466.4	331.5
benzyl-phenyl ether	142.2 ± 1.1	456.9	314.7
1,3-diphenyl-propane	140.9 ± 2.5	498.9	358.0
dibenzyl ether	151.8 ± 1.3	502.4	350.6
naphthalene			217.6 [46]
2-methoxy-naphthalene	137.9 ± 1.6	401.5	263.6
cyclohexane			204.4 [47]
methoxy–cyclohexane	106.7 ± 3.2 [48]	376.8	270.1
dicyclohexyl-methane	136.3 ± 2.8 [34]	470.5	334.2
1,2-dicyclohexyl-ethane	137.1 ± 2.6	510.5	373.4
1,3-dicayclohexyl-propane	144.1 ± 1.7	544.4	400.3
dicyclohexyl ether	142.9 ± 3.9	475.1	332.2
cyclohexylmethoxy–cyclohexane	145.0 ± 5.0 [d]	511.1	366.1
dicyclohexylmethyl ether	147.9 ± 7.1	539.2	391.3
trans-decalin			264.9 [49]
2-methoxy-decalin	123.8 ± 5.7	446.3	322.5

[a] From the results, the vapour pressure measurements are compiled in Tables S3 and S4. [b] Calculated with the G3MP2 method. [c] Calculated according to Equation (14) using entries from columns 2 and 3 from this table. [d] Assessed. The changes in the standard molar entropies of the dehydrogenation reactions R1 to R10 were calculated according to Equation (12) using the standard molar entropies of the reactants from Table 7, as follows.

Table 8. Liquid-phase thermodynamic properties of the dehydrogenation of LOHC systems.

Reactants	$\Delta_r H_m^o$ [a] (298 K)	$\Delta_r S_m^o$ [b] (298 K)	$T \times \Delta_r S_m^o$ (298 K)	$\Delta_r G_m^o$ [c] (298 K)	$\Delta_r G_m^o$ [d] (400 K)	$\Delta_r G_m^o$ [e] (500 K)
	kJ·mol^{-1}	J·mol^{-1}·K^{-1}	kJ·mol^{-1}	kJ·mol^{-1}	kJ·mol^{-1}	kJ·mol^{-1}
benzene	205.4	360.9	107.6	97.8	60.1	21.1
cyclohexane	**68.5**	**120.3**	**35.9**	**32.6**	**20.0**	**7.0**
methoxy–benzene	197.7	356.7	106.4	91.3	23.9	14.6
methoxy–cyclohexane	**65.9**	**118.9**	**35.5**	**30.4**	**18.0**	**4.9**
diphenyl–methane	403.7	749.7	223.5	180.2	102.2	22.1
dicyclohexyl–methane	**67.3**	**125.0**	**37.3**	**30.0**	**17.0**	**3.7**
diphenyl–ether	408.5	757.2	225.8	182.7	103.8	22.5
dicyclohexyl ether	**68.1**	**126.2**	**37.6**	**30.5**	**17.3**	**3.8**
1,2-diphenyl-ethane	393.2	742.2	221.3	171.9	94.5	14.5
1,2-dicyclohexyl-ethane	**65.5**	**123.7**	**36.9**	**28.7**	**15.7**	**2.4**
benzyl phenyl ether	398.6	732.7	218.5	180.2	103.6	24.3
Cyclohexylmethoxy–cyclohexane	**66.4**	**122.1**	**36.4**	**30.0**	**17.3**	**4.1**
1,3-diphenyl-propane	394.8	741.8	221.2	173.6	96.2	16.3
1,3-dicyclohexyl-propane	**65.8**	**123.6**	**36.9**	**28.9**	**16.0**	**2.7**
dibenzyl ether	409.8	743.4	221.6	188.2	110.5	30.2
dicyclohexylmethyl ether	**68.3**	**123.9**	**36.9**	**31.4**	**18.4**	**5.0**

Table 8. *Cont.*

Reactants	$\Delta_r H_m^o$ [a] (298 K)	$\Delta_r S_m^o$ [b] (298 K)	$T \times \Delta_r S_m^o$ (298 K)	$\Delta_r G_m^o$ [c] (298 K)	$\Delta_r G_m^o$ [d] (400 K)	$\Delta_r G_m^o$ [e] (500 K)
naphthalene	325.5	606.1	180.7	144.8	81.4	15.7
trans-decalin	**65.1**	**121.2**	**36.1**	**29.0**	**16.3**	**3.1**
2-methoxy-naphthalene	312.2	594.5	177.3	134.9	72.8	8.2
trans-2-methoxy-decalin	**62.4**	**118.9**	**35.5**	**27.0**	**14.6**	**1.6**

[a] Calculated according to Equation (11) from standard molar enthalpies of formation of reactants from Table 6. Values highlighted in bold are related to the amount of hydrogen released and given in $kJ \cdot mol^{-1}/_{H2}$ units. More details are shown in Table S13. [b] Calculated according to Equation (12) from standard molar entropies of reactants from Table 7. Values highlighted in bold are related to the amount of hydrogen released and given in $J \cdot mol^{-1} \cdot K^{-1}/_{H2}$ units. [c] Calculated according to Equation (1) from results given in columns 2 and 3 and referenced to 298 K. [d] The $\Delta_r G_m^o$(298.15 K) value from column 4 was adjusted to 400 K, as shown in ESI. [e] The $\Delta_r G_m^o$(298.15 K) value from column 4 was adjusted to 500 K, as shown in ESI.

As can be seen from Table 8, the reaction entropies of R1 to R10 are between 357 and 757 $J \cdot mol^{-1} \cdot K^{-1}$. For an appropriate comparison, however, they should also be related to the amount of hydrogen released, whereby the stoichiometry must be taken into account. As shown in Table 8, the dehydrogenation entropies in all LOHC pairs are barely distinguishable at the level of ≈ 120 $J \cdot mol^{-1} \cdot K^{-1}/_{H2}$, and this observation is important for chemical engineering calculations with the LOHC systems. As also shown in Table 8, the entropy contributions ($T \times \Delta_r S_m^o$) to the Gibbs energy of the reactions R1 to R10 very close for all reactions on the level of ≈ 36 $J \cdot mol^{-1} \cdot K^{-1}$. From a thermodynamic point of view, the equilibrium position for these reactions is, therefore, mainly determined by the enthalpic term. Thus, both the required enthalpic ($\Delta_f H_m^o$(liq, 298.15 K) and entropic $\Delta_r S_m^o$(liq, 298.15 K) contributions to the Gibbs–Helmholtz equation (Equation (1)) have now been developed and are ready for the comparison of the Gibbs energies of the dehydrogenation reactions R1 to R10 in the following section.

3.3.3. Comparison of the Gibbs Energies of Dehydrogenation Reactions R1 to R10

The total liquid-phase Gibbs energies and equilibrium constants of dehydrogenation reactions R1 to R10 calculated according to Equation (1) are given in Table 9.

Table 9. The total Gibbs free reaction enthalpies (in $kJ \cdot mol^{-1}$) and equilibrium constants of dehydrogenation of aliphatic cyclic hydrocarbons and ethers in the liquid phase, calculated according to Equation (1).

LOHC System	$\Delta_r G_m^o$ (298 K)	$\Delta_r G_m^o$ (400 K)	$\Delta_r G_m^o$ (500 K)	K_a (298 K)	K_a (400 K)	K_a (500 K)
cyclohexane	97.8	60.1	21.1	7.2×10^{-18}	1.4×10^{-8}	6.2×10^{-3}
methoxy–cyclohexane	91.3	23.9	14.6	9.9×10^{-17}	7.6×10^{-4}	3.0×10^{-2}
dicyclohexyl–methane	180.2	102.2	22.1	2.6×10^{-32}	4.5×10^{-14}	4.9×10^{-3}
dicyclohexyl ether	182.7	103.8	22.5	9.4×10^{-33}	2.8×10^{-14}	4.5×10^{-3}
1,2-dicyclohexyl-ethane	171.9	94.5	14.5	7.4×10^{-31}	4.6×10^{-13}	3.1×10^{-2}
Cyclohexylmethoxy–cyclohexane	180.2	103.6	24.3	2.6×10^{-32}	3.0×10^{-14}	2.9×10^{-3}
1,3-dicyclohexyl-propane	173.6	96.2	16.3	3.7×10^{-31}	2.7×10^{-13}	2.0×10^{-2}
dicyclohexylmethyl ether	188.2	110.5	30.2	1.0×10^{-33}	3.7×10^{-15}	7.0×10^{-4}
decalin	144.8	81.4	15.7	4.1×10^{-26}	2.3×10^{-11}	2.3×10^{-2}
2-methoxy-decalin	134.9	72.8	8.2	2.3×10^{-24}	3.1×10^{-10}	1.4×10^{-1}

As shown in Table 9, the $\Delta_r G_m^o$ values for all pairs of LOHC molecules are positive and strongly temperature-dependent. The oxygen functionality significantly decreases the $\Delta_r G_m^o$ values for pairs methoxy–cyclohexane/methoxy–benzene and 2-methoxy-decalin/2-methoxy-naphthalene. For the system dicyclohexyl/diphenyl ether, the introduction of oxygen instead of the methylene group does not change the energetics practically. For systems cyclohexylmethoxy–cyclohexane/benzyl phenyl ether and dicyclohexylmethyl ether/dibenzylether, the oxygen functionality even increases the $\Delta_r G_m^o$ values (compared to the similarly shaped hydrocarbons), making the thermodynamics of these LOHC systems even less favourable.

The influence of the oxygen functionality becomes clearer when comparing the equilibrium constants K_a (e.g., at 500 K), as the size of the equilibrium constant is directly related to the amount of the compound with a low hydrogen content in the reaction mixture of the dehydrogenation reaction. For example, for the methoxy–cyclohexane/methoxy–benzene pair, the constant $K_a = 3.0 \times 10^{-2}$ (see Table 9, last column) is approximately an order of magnitude greater than the constant $K_a = 6.2 \times 10^{-3}$ (see Table 9, last column) for the cyclohexane/benzene pair.

For the 2-methoxy-decalin/2-methoxy-naphthalene pair, the constant $K_a = 1.4 \times 10^{-1}$ (see Table 9, last column) is also an order of magnitude greater than the constant $K_a = 2.3 \times 10^{-2}$ (see Table 9, last column) for the decalin/naphthalene pair. For the dicyclohexyl/diphenyl ether system, the constant $K_a = 4.5 \times 10^{-3}$ (see Table 9, last column) is about the same as the constant $K_a = 4.9 \times 10^{-3}$ (see Table 9, last column) for the dicyclohexyl–methane/diphenyl–methane system and the introduction of oxygen instead of the methylene group practically does not change the energetics. In the cyclohexylmethoxy–cyclohexane/benzylphenyl ether and dicyclohexylmethyl ether/dibenzyl ether systems, the oxygen functionality reduces the K_a values compared to the corresponding hydrocarbon-based LOHC systems.

3.3.4. Thermodynamic Analysis of the Reversible Hydrogenation/Dehydrogenation Process in the Gas Phase

Admittedly, the hydrogen release from the hydrogen-rich LOHC counterparts is a thermodynamically unfavourable process [1]. However, a theoretical optimal dehydrogenation temperature can be evaluated based on quantum chemical calculations of the Gibbs free energy according to Equation (1). If the system approximates the equilibrium, the free reaction energy approaches zero. A theoretically optimal dehydrogenation temperature can be determined on the basis of quantum chemical calculations of the Gibbs free energy according to Equation (1). When the system approaches equilibrium, the free energy of the reaction approaches zero. When the $\Delta_r G_m^o = 0$, the enthalpy term $\Delta_r H_m^o$ and the entropy term $T \times \Delta_r S_m^o$ in Equation (1) become equal. This occurs at a certain "equilibrium temperature", T_{eq}, which can imply the reversal of thermodynamic feasibility from dehydrogenation to hydrogenation tendency:

$$T_{eq} = \frac{\Delta_r H_m^o}{\Delta_r S_m^o} \tag{13}$$

This temperature can be considered a valuable indicator for selecting the optimum temperature for a particular LOHC system. This T_{eq} for the dehydrogenation step should not be too high, but sufficient to achieve good conversion and selectivity. For the hydrogenation step, the T_{eq} should not be too low in order to achieve acceptable reaction rates. The results of the T_{eq} calculations according to Equation (13) for the reactions R1 to R10 are compared in Table 10.

As can be seen from Table 10, the T_{eq} values for dehydrogenation in LOHC systems based on aliphatic cyclic hydrocarbons vary between 530 and 569 K. The T_{eq} values for dehydrogenation in aliphatic cyclic ethers are generally somewhat lower and vary between 525 and 554 K. The lowest equilibrium temperature is observed for trans-2-methoxydecaline (525 K). However, the positive influence of the oxygen function is only significant for

methoxy–cyclohexane and trans-2-methoxy-decaline. For other pairs, the T_{eq} values are slightly higher for oxygen-containing compounds (see Table 10).

Table 10. Calculation of the equilibrium temperature, T_{eq}, for dehydrogenation/hydrogenation reactions with aliphatic cyclic hydrocarbons and ethers in the liquid phase calculated using the G3MP2 method ($p° = 0.1$ MPa).

Reactants	$\Delta_r H_m^o$ [a]	$\Delta_r S_m^o$ [b]	T_{eq} [c]
	kJ·mol^{-1}	J·mol^{-1}·K^{-1}	K
cyclohexane = benzene + 3 × H$_2$	205.4	360.9	569
methoxy–cyclohexane = methoxy–benzene + 3 × H$_2$	197.7	356.7	554
Dicyclohexyl–methane = diphenyl–methane + 6 × H$_2$	403.7	749.7	538
dicyclohexyl ether = diphenyl ether + 6 × H$_2$	408.5	757.2	539
1,2-dicyclohexyl-ethane = 1,2-diphenyl-ethane + 6 × H$_2$	393.2	742.2	530
cyclohexylmethoxy–cyclohexane = benzyl phenyl ether + 6 × H$_2$	398.6	732.7	544
1,3-dicyclohexyl-propane = 1,3-diphenyl-propane + 6 × H$_2$	394.8	741.8	532
dibenzyl ether + 6 × H$_2$ = dicyclohexylmethyl ether	409.8	743.4	551
trans-decalin = naphthalene + 5 × H$_2$	325.5	606.1	537
trans-2-methoxy-decalin = 2-methoxy-naphthalene + 5 × H$_2$	312.2	594.5	525

[a] The total reaction enthalpies from Table 9. [b] The total reaction entropies from Table 9. [c] The equilibrium temperature calculated according to Equation (13).

4. Conclusions

The thermodynamic properties of a series of aromatic ethers have been studied using different experimental and theoretical methods in order to evaluate their applicability as LOHC materials. The consistent sets of phase transition enthalpies and entropies, enthalpies of formation, and absolute entropies were obtained using vapour pressure measurements, combustion calorimetry, and empirical and quantum chemical calculations. These results were recommended for chemical engineering calculations to optimise the storage and release of hydrogen using the reversible hydrogenation/dehydrogenation reactions. The thermodynamic properties of the liquid-phase hydrogenation/dehydrogenation reactions in LOHC systems based on methoxy–benzene, diphenyl ether, benzyl phenyl ether, dibenzyl ether, and 2-methoxy-naphthalene were derived and compared with the data for the similarly structured hydrogen carriers based on benzene, diphenyl-methane, 1,2-diphenyl-ethane, 1,3-diphenyl-propane and naphthalene. The effects of oxygen functionality on the thermodynamic properties of hydrogenation/dehydrogenation reactions were evaluated. It was found that for methoxy–benzene and 2-methoxy-naphthalene, a reduction in enthalpies and Gibbs-free energies for the dehydrogenation reactions can be observed, allowing more favourable reaction conditions to be achieved. For systems based on diphenyl ether, the thermodynamic properties of the reaction are very similar to those of the diphenyl–methane system. In the systems based on benzyl phenyl ether and dibenzyl ether, the introduction of oxygen functionality is not advantageous compared to LOHC systems based on 1,2-diphenylethane and 1,3-diphenylpropane. These new findings contribute to a better understanding of the reaction thermodynamic properties of LOHC systems and reveal the structural features of aromatic and aliphatic cyclic compounds that are essential for their technical applications. Further investigation of the thermodynamic properties of hydrogenation/dehydrogenation reactions for LOHC systems containing one or two oxygen functions in the aliphatic ring should complete this interesting structure–property evaluation.

Supplementary Materials: The following supporting information can be downloaded at: https://www.mdpi.com/article/10.3390/oxygen4030015/s1, Figure S1: The development of the contributions C6H5- (left) and C6H11- (right) for calculating the vaporization enthalpies (or gas-phase enthalpies of formation) of aromatic and cyclic aliphatic hydrocarbons using the GA method. All values in kJ·mol^{-1}. The numerical values of the contributions are given in Table S8. Results of calculations are shown in Table S9; Figure S2: The most stable conformers for the aromatic compounds and their perhydrogenated products; Table S1: Provenance and purity of the materials; Table S2: Auxiliary quantities: formula, density ρ(293 K), massic heat capacity c_p(298.15 K), and expansion coefficients $(\delta V/\delta T)_p$ of the materials used in the present study; Table S3: Absolute vapour pressures p, and standard molar vaporisation enthalpies and entropies determined using the transpiration method; Table S4: The vapour pressures p, and standard vaporisation enthalpies and entropies obtained by the approximation of boiling points at different pressures available in the literature; Table S5: Enthalpies of fusion ($\Delta_{cr}^{l}H_m^{o}$), vaporization ($\Delta_{l}^{g}H_m^{o}$) and sublimation ($\Delta_{cr}^{g}H_m^{o}$) at melting points (T_{fus}) and at 298.15 K of benzyl phenyl ether and 2-methoxy-naphthalene; Table S6: Compilation of data on molar heat capacities $C_{p,m}^{o}$(liq) and heat capacity differences $\Delta_{l}^{g}C_{p,m}^{o}$ (in J·K^{-1}·mol^{-1}) at T = 298.15 K; Table S7: Coefficients of the Clarke and Glew equation (S6) for 1,2-diphenyl-ethane from Osborn et al; Table S8: Group-additivity values Γ_i for calculation of enthalpies of vaporization, $\Delta_{l}^{g}H_m^{o}$, and enthalpies of formation, $\Delta_f H_m^{o}$(g), of alkanes, ethers, and aromatics at 298.15 K in kJ mol^{-1}; Table S9: Comparison of experimental thermochemical data with those calculated by group additivity at T = 298.15 K (p° = 0.1 MPa) for ethers and hydrocarbons (in kJ·mol^{-1}); Table S10: Calculation of the G3MP2 *corrected* gas-phase enthalpies at T = 298.15 K (in kJ·mol^{-1}); Table S11: Comparison of experimental and G3MP2 calculated gas-phase enthalpies of formation for alkyl-cyclohexanes (at T = 298.15 K, p° = 0.1 MPa, in kJ·mol^{-1}); Table S12: Thermochemical data at T = 298.15 K (p° = 0.1 MPa) for auxiliary compounds (in kJ·mol^{-1}); Table S13: Liquid phase thermodynamic properties of the hydrogenation of the hydrogen-lean LOHC counterparts.

Institutional Review Board Statement: Not applicable.

Informed Consent Statement: Not applicable.

Data Availability Statement: The original contributions presented in the study are included in the article/supplementary material, further inquiries can be directed to the corresponding author/s.

Conflicts of Interest: The authors declare no conflict of interest.

References

1. Preuster, P.; Papp, C.; Wasserscheid, P. Liquid Organic Hydrogen Carriers (LOHCs): Toward a Hydrogen-Free Hydrogen Economy. *Acc. Chem. Res.* **2017**, *50*, 74–85. [CrossRef] [PubMed]
2. Hodoshima, S.; Takaiwa, S.; Shono, A.; Satoh, K.; Saito, Y. Hydrogen Storage by Decalin/Naphthalene Pair and Hydrogen Supply to Fuel Cells by Use of Superheated Liquid-Film-Type Catalysis. *Appl. Catal. A Gen.* **2005**, *283*, 235–242. [CrossRef]
3. Sebastián, D.; Bordejé, E.G.; Calvillo, L.; Lázaro, M.J.; Moliner, R. Hydrogen Storage by Decalin Dehydrogenation/Naphthalene Hydrogenation Pair over Platinum Catalysts Supported on Activated Carbon. *Int. J. Hydrogen Energy* **2008**, *33*, 1329–1334. [CrossRef]
4. Sung, J.; Choo, K.; Kim, T.; Tarasov, A.; Tkachenko, O.; Kustov, L. A New Hydrogen Storage System Based on Efficient Reversible Catalytic Hydrogenation/Dehydrogenation of Terphenyl. *Int. J. Hydrogen Energy* **2008**, *33*, 2721–2728. [CrossRef]

5. Kustov, L.M.; Kalenchuk, A.N.; Bogdan, V.I. Systems for Accumulation, Storage and Release of Hydrogen. *Russ. Chem. Rev.* **2020**, *89*, 897–916. [CrossRef]

6. Pez, G.P.; Scott, A.R.; Cooper, A.C.; Cheng, H.; Wilchelm, F.C.; Abdourazak, A.H. Hydrogen storage by reversible hydrogenation of pi-conjugated substrates. US patent US7351395B1, 2008. Available online: https://patents.google.com/patent/US7351395B1/en (accessed on 26 June 2024).

7. Bourane, A.; Elanany, M.; Pham, T.V.; Katikaneni, S.P. An Overview of Organic Liquid Phase Hydrogen Carriers. *Int. J. Hydrogen Energy* **2016**, *41*, 23075–23091. [CrossRef]

8. Cooper, A.C.; Campbell, K.M.; Pez, G.P. An Integrated Hydrogen Storage and Delivery Approach Using Organic Liquid-Phase Carriers. In Proceedings of the 16th World Hydrogen Energy Conference 2006, Lyon, France, 13–16 June 2006; Volume 3, pp. 2164–2175.

9. Products, A.; Cooper, A.C.; Manager, P. *Design and Development of New Carbon-Based Sorbent Systems for an Effective Containment of Hydrogen Final Report Revised April 2012 Hydrogen Storage by Reversible Hydrogenation of Solid- and Liquid-Phase Hydrogen Carriers*; Air Products and Chemicals, Inc.: Allentown, PA, USA, 2012.

10. Crabtree, R.H. Hydrogen Storage in Liquid Organic Heterocycles. *Energy Environ. Sci.* **2008**, *1*, 134. [CrossRef]

11. Zakgeym, D.; Hofmann, J.D.; Maurer, L.A.; Auer, F.; Müller, K.; Wolf, M.; Wasserscheid, P. Better through Oxygen Functionality? The Benzophenone/Dicyclohexylmethanol LOHC-System. *Sustain. Energy Fuels* **2023**, *7*, 1213–1222. [CrossRef]

12. Emel'yanenko, V.N.; Zaitseva, K.V.; Agapito, F.; Martinho Simões, J.A.; Verevkin, S.P. Benchmark Thermodynamic Properties of Methylanisoles: Experimental and Theoretical Study. *J. Chem. Thermodyn.* **2015**, *85*, 155–162. [CrossRef]

13. Verevkin, S.P.; Zaitsau, D.H.; Emel'yanenko, V.N.; Zhabina, A.A. Thermodynamic Properties of Glycerol: Experimental and Theoretical Study. *Fluid Phase Equilib.* **2015**, *397*, 87–94. [CrossRef]

14. Verevkin, S.P.; Emel'yanenko, V.N.; Diky, V.; Muzny, C.D.; Chirico, R.D.; Frenkel, M. New Group-Contribution Approach to Thermochemical Properties of Organic Compounds: Hydrocarbons and Oxygen-Containing Compounds. *J. Phys. Chem. Ref. Data* **2013**, *42*, 033102. [CrossRef]

15. Emel'yanenko, V.N.; Verevkin, S.P.; Heintz, A. The Gaseous Enthalpy of Formation of the Ionic Liquid 1-Butyl-3-Methylimidazolium Dicyanamide from Combustion Calorimetry, Vapor Pressure Measurements, and Ab Initio Calculations. *J. Am. Chem. Soc.* **2007**, *129*, 3930–3937. [CrossRef] [PubMed]

16. Verevkin, S.P.; Emel'yanenko, V.N. Transpiration Method: Vapor Pressures and Enthalpies of Vaporization of Some Low-Boiling Esters. *Fluid Phase Equilib.* **2008**, *266*, 64–75. [CrossRef]

17. Emel'yanenko, V.N.; Zaitsau, D.H.; Shoifet, E.; Meurer, F.; Verevkin, S.P.; Schick, C.; Held, C. Benchmark Thermochemistry for Biologically Relevant Adenine and Cytosine. A Combined Experimental and Theoretical Study. *J. Phys. Chem. A* **2015**, *119*, 9680–9691. [CrossRef] [PubMed]

18. Pracht, P.; Bohle, F.; Grimme, S. Automated Exploration of the Low-Energy Chemical Space with Fast Quantum Chemical Methods. *Phys. Chem. Chem. Phys.* **2020**, *22*, 7169–7192. [CrossRef] [PubMed]

19. Petersson, G.A.; Bennett, A.; Tensfeldt, T.G.; Al-Laham, M.A.; Shirley, W.A.; Mantzaris, J. A Complete Basis Set Model Chemistry. I. The Total Energies of Closed-shell Atoms and Hydrides of the First-row Elements. *J. Chem. Phys.* **1988**, *89*, 2193–2218. [CrossRef]

20. Frisch, M.J.; Trucks, G.W.; Schlegel, H.B.; Scuseria, G.E.; Robb, M.A.; Cheeseman, J.R.; Scalmani, G.; Barone, V.; Petersson, G.A.; Nakatsuji, H.; et al. *Gaussian 16, Revision C.01*; Gaussian, Inc.: Wallingford, CT, USA, 2016.

21. Curtiss, L.A.; Raghavachari, K.; Redfern, P.C.; Pople, J.A. Gaussian-3 Theory Using Scaled Energies. *J. Chem. Phys.* **2000**, *112*, 1125–1132. [CrossRef]

22. Verevkin, S.P.; Emel'yanenko, V.N.; Notario, R.; Roux, M.V.; Chickos, J.S.; Liebman, J.F. Rediscovering the Wheel. Thermochemical Analysis of Energetics of the Aromatic Diazines. *J. Phys. Chem. Lett.* **2012**, *3*, 3454–3459. [CrossRef] [PubMed]

23. Olofsson, G. Assignment of Uncertainties. In *Combustion Calorimetry: Experimental Chemical Thermodynamics*; Sunner, S., Månsson, M., Eds.; Pergamon: New York, NY, USA, 1979; pp. 137–161.

24. Cox, J.D.; Wagman, D.D.; Medvedev, V.A. *CODATA Key Values for Thermodynamics: Final Report of the CODATA Task Group on Key Values for Thermodynamics*; CODATA Series on Thermodynamic; Hemisphere Publishing Corp.: New York, NY, USA, 1989.

25. Hubbard, W.N.; Scott, D.W.; Waddington, G. Standard States and Corrections for Combustions in a Bomb at Constant Volume. In *Experimental Thermochemistry*; Rossini, F.D., Ed.; Interscience Publishers: New York, NY, USA, 1956; pp. 75–128.

26. Stull, D.R. Vapor Pressure of Pure Substances. Organic and Inorganic Compounds. *Ind. Eng. Chem.* **1947**, *39*, 517–540. [CrossRef]

27. Stephenson, R.M.; Malanowski, S. *Handbook of the Thermodynamics of Organic Compounds*; Springer: Dordrecht, The Netherlands, 1987; ISBN 978-94-010-7923-5.

28. Barontini, F.; Cozzani, V. Thermogravimetry as a Screening Tool for the Estimation of the Vapor Pressures of Pure Compounds. *J. Therm. Anal. Calorim.* **2007**, *89*, 309–314. [CrossRef]

29. Emel'yanenko, V.N.; Zaitsau, D.H.; Pimerzin, A.A.; Verevkin, S.P. Benchmark Properties of Diphenyl Oxide as a Potential Liquid Organic Hydrogen Carrier: Evaluation of Thermochemical Data with Complementary Experimental and Computational Methods. *J. Chem. Thermodyn.* **2018**, *125*, 149–158. [CrossRef]

30. Osborn, A.G.; Scott, D.W. Vapor Pressures of 17 Miscellaneous Organic Compounds. *J. Chem. Thermodyn.* **1980**, *12*, 429–438. [CrossRef]

31. Bolmatenkov, D.N.; Yagofarov, M.I.; Notfullin, A.A.; Solomonov, B.N. Calculation of the Vaporization Enthalpies of Alkylaromatic Hydrocarbons as a Function of Temperature from Their Molecular Structure. *Fluid Phase Equilib.* **2022**, *554*, 113303. [CrossRef]

32. Verevkin, S.P.; Samarov, A.A.; Vostrikov, S. V Thermodynamics of Reversible Hydrogen Storage: Does Alkoxy-Substitution of Naphthalene Yield Functional Advantages for LOHC Systems? *J. Chem. Phys.* **2024**, *160*, 154709. [CrossRef] [PubMed]

33. Samarov, A.A.; Verevkin, S.P. Hydrogen Storage Technologies: Methyl-Substituted Biphenyls as an Auspicious Alternative to Conventional Liquid Organic Hydrogen Carriers (LOHC). *J. Chem. Thermodyn.* **2022**, *165*, 106648. [CrossRef]

34. Verevkin, S.P.; Samarov, A.A.; Vostrikov, S.V.; Wasserscheid, P.; Müller, K. Comprehensive Thermodynamic Study of Alkyl-Cyclohexanes as Liquid Organic Hydrogen Carriers Motifs. *Hydrogen* **2023**, *4*, 42–59. [CrossRef]

35. Benson, S.W. *Thermochemical Kinetics*, 2nd ed.; John Wiley & Sons: New York, NY, USA; London, UK; Sydney, Australia; Toronto, ON, Canada, 1976; pp. 1–320.

36. Verevkin, S.P.; Emel'yanenko, V.N.; Pimerzin, A.A.; Vishnevskaya, E.E. Thermodynamic Analysis of Strain in the Five-Membered Oxygen and Nitrogen Heterocyclic Compounds. *J. Phys. Chem. A* **2011**, *115*, 1992–2004. [CrossRef]

37. Steele, W.V.; Chirico, R.D.; Knipmeyer, S.E.; Nguyen, A.; Smith, N.K.; Tasker, I.R. Thermodynamic Properties and Ideal-Gas Enthalpies of Formation for Cyclohexene, Phthalan (2,5-Dihydrobenzo-3,4-Furan), Isoxazole, Octylamine, Dioctylamine, Trioctylamine, Phenyl Isocyanate, and 1,4,5,6-Tetrahydropyrimidine. *J. Chem. Eng. Data* **1996**, *41*, 1269–1284. [CrossRef]

38. Chirico, R.; Archer, D.; Hossenlopp, I.; Nguyen, A.; Steele, W.; Gammon, B. The Thermodynamic Properties of Chroman and Isochroman. *J. Chem. Thermodyn.* **1990**, *22*, 665–682. [CrossRef]

39. Wheeler, S.E.; Houk, K.N.; Schleyer, P.v.R.; Allen, W.D. A Hierarchy of Homodesmotic Reactions for Thermochemistry. *J. Am. Chem. Soc.* **2009**, *131*, 2547–2560. [CrossRef]

40. Verevkin, S.P.; Vostrikov, S.V.; Leinweber, A.; Wasserscheid, P.; Müller, K. Thermochemical Properties of Benzyltoluenes and Their Hydro- and Perhydro-Derivatives as Key Components of a Liquid Organic Hydrogen Carrier System. *Fuel* **2023**, *335*, 126618. [CrossRef]

41. Roux, M.V.; Temprado, M.; Chickos, J.S.; Nagano, Y. Critically Evaluated Thermochemical Properties of Polycyclic Aromatic Hydrocarbons. *J. Phys. Chem. Ref. Data* **2008**, *37*, 1855–1996. [CrossRef]

42. Pedley, J.B.; Naylor, R.D.; Kirby, S.P. *Thermochemical Data of Organic Compounds*; Chapman and Hall: New York, NY, USA, 1986; pp. 1–792.

43. Oliver, G.D.; Eaton, M.; Huffman, H.M. The Heat Capacity, Heat of Fusion and Entropy of Benzene 1. *J. Am. Chem. Soc.* **1948**, *70*, 1502–1505. [CrossRef]

44. Ambrose, D.; Ellender, J.; Sprake, C.H.; Townsend, R. Thermodynamic Properties of Organic Oxygen Compounds XLIII. Vapour Pressures of Some Ethers. *J. Chem. Thermodyn.* **1976**, *8*, 165–178. [CrossRef]

45. Chirico, R.D.; Steele, W.V. Thermodynamic Properties of Diphenylmethane. *J. Chem. Eng. Data* **2005**, *50*, 1052–1059. [CrossRef]

46. Chirico, R.D.; Knipmeyer, S.E.; Nguyen, A.; Steele, W.V. The Thermodynamic Properties to the Temperature 700 K of Naphthalene and of 2,7-Dimethylnaphthalene. *J. Chem. Thermodyn.* **1993**, *25*, 1461–1494. [CrossRef]

47. Ruehrwein, R.A.; Huffman, H.M. Thermal Data. XVII. The Heat Capacity, Entropy, and Free Energy of Formation of Cyclohexane. A New Method of Heat Transfer in Low Temperature Calorimetry. *J. Am. Chem. Soc.* **1943**, *65*, 1620–1625. [CrossRef]

48. Verevkin, S.P.; Samarov, A.A.; Vostrikov, S.V. Thermodynamics of Reversible Hydrogen Storage: Are Methoxy-Substituted Biphenyls Better through Oxygen Functionality? *Hydrogen* **2023**, *4*, 862–880. [CrossRef]

49. McCullough, J.P.; Finke, H.L.; Messerly, J.F.; Todd, S.S.; Kincheloe, T.C.; Waddington, G. The Low-Temperature Thermodynamic Properties of Naphthalene, l-Methylnaphthalene, 2-Methylnaphthalene, 1,2,3,4-Tetrahydronaphthalene,Trans-Decahydronaphthalene and Cis-Decahydronaphthalene. *J. Phys. Chem.* **1957**, *61*, 1105–1116. [CrossRef]